Excitation of nonlinear second order betatron sidebands for Knock Out slow extraction at the 1/3 resonance

Philipp Niedermayer * and Rahul Singh
GSI Helmholtzzentrum für Schwerionenforschung, Darmstadt, Germany
(Dated: April 18, 2024)

Radio Frequency Knock Out resonant slow extraction is a standard method for extracting stored particle beams from synchrotrons by transverse excitation. Classically, the beam is excited with an RF field comprising a frequency band around one of the betatron sidebands. This article demonstrates that the 1/3 resonance commonly used for the slow extraction induces nonlinear motion, resulting in the appearance of additional sidebands of higher order at multiples of the betatron tune. Measured and simulated beam spectra are presented, revealing these sidebands and the beam's response to being excited at first and second order sidebands. The feasibility of using a second order sideband for the purpose of slow extraction is demonstrated. This results in a significant improvement in the temporal structure (spill quality) of the extracted beam, but at the cost of higher excitation power requirements. This is observed both experimentally and in tracking simulations. The mechanism behind the observed improvement is explained using beam dynamics simulations.

I. INTRODUCTION

Radio Frequency Knock Out (RF-KO) resonant slow extraction is used to extract stored particle beams from synchrotron rings [1, 2]. Therefore, a beam optics near a third order resonance is chosen where sextupole fields create a transverse, betatron amplitude dependent instability (separatrix) [3]. For storing and accelerating a beam such instabilities are undesired and investigated to be corrected [4]; but in the context of slow extraction they are exploited and enhanced by dedicated sextupole magnets. The beam is driven into the instability in a controlled manner by increasing the particle amplitude through transverse excitation. The excitation system consists of a radio frequency (RF) signal generator, RF amplifiers, and a stripline kicker [5], inside of which electromagnetic RF fields deflect traversing particles on each turn. When particles reach the separatrix, their motion becomes unbound and the betatron amplitude increases rapidly, such that septa can be used to deflect the extracted particles into an extraction beam line. This *spill* of extracted particles is then delivered to experiments or medical therapy.

A. Nonlinear betatron oscillation

With the working point (tune) of the circular accelerator close to a 1/3 resonance and nonlinear sextupole fields driving the resonance, the three-turn particle dynamics is described by the Kobayashi Hamiltonian [6]

$$\begin{aligned} H &= 3\pi d \left(X^2 + X'^2\right) + \frac{S}{4}\left(3XX'^2 - X^3\right) \\ &= 6\pi d J_\mathrm{x} - \frac{S}{\sqrt{2}} J_\mathrm{x}^{3/2}\cos(3\Theta_\mathrm{x}) \end{aligned}$$

where $S = -\beta_x(s)^{3/2} k_2 l/2$ is the normalized sextupole strength and

$$\begin{aligned} X &= \sqrt{2J_\mathrm{x}}\cos(\Theta_\mathrm{x}) = \frac{1}{\sqrt{\beta_\mathrm{x}(s)}}\,x(s) \\ X' &= -\sqrt{2J_\mathrm{x}}\sin(\Theta_\mathrm{x}) = -\frac{\beta_\mathrm{x}'(s)}{2\sqrt{\beta_\mathrm{x}(s)}}\,x(s) + \sqrt{\beta_\mathrm{x}(s)}\,x'(s) \end{aligned}$$

are the normalized phase space coordinates with the action J_x and angle Θ_x [3]. The relation to the physical coordinate[1] x and divergence x' is thereby given by the beta function $\beta_\mathrm{x}(s)$ which describes the optical properties of the lattice at the location s. The (small) quantity $d = Q_\mathrm{x} - Q_\mathrm{res}$ is the distance of the tune[2] Q_x to the 1/3 resonance Q_res with $3Q_\mathrm{res} \in \mathbb{N}$. In the following, uppercase symbols will be used to denote absolute tune values, while the lowercase $q \leq 0.5$ refers to the fractional tune as distance to the nearest integer.

In the linear case ($S = 0$) particles perform harmonic betatron oscillations with a constant phase advance per turn $\mu_1 = 2\pi Q_\mathrm{x}$. Near the resonance, however, the betatron oscillations becomes nonlinear and the sextupole field causes an amplitude and phase dependent detuning. In thin lens and flat beam approximation, the kick induced by the sextupole is $\Delta X' = SX^2$. For the angle after the sextupole one can thus write

$$\tan(\Theta_{\mathrm{x},1}) = -\frac{X' + SX^2}{X} = \tan(\Theta_\mathrm{x}) - S\sqrt{2J_\mathrm{x}}\cos(\Theta_\mathrm{x})$$

Considering that the sextupole kick is small and using the small angle approximation

$$\tan(\Theta_\mathrm{x} + \Delta\Theta_\mathrm{x}) \approx \tan(\Theta_\mathrm{x}) + \frac{\Delta\Theta_\mathrm{x}}{\cos^2(\Theta_\mathrm{x})} + \mathcal{O}\left(\Delta\Theta_\mathrm{x}^2\right)$$

* p.niedermayer@gsi.de

[1] Corrected for closed orbit and dispersion
[2] Including chromatic detuning: $Q_\mathrm{x} = Q_{\mathrm{x,ref}} + \xi_\mathrm{x}\delta$

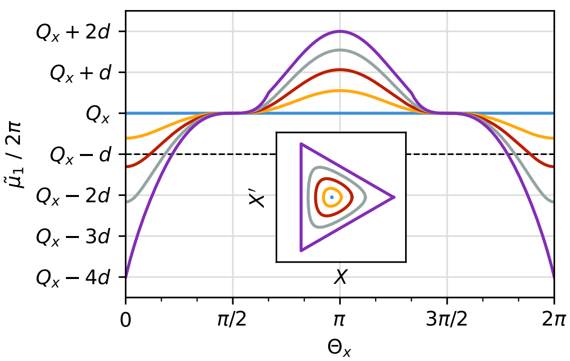

FIG. 1. Nonlinear detuning of the phase advance per turn as function of angle, calculated for different values of the Hamiltonian H. The dashed line marks the resonance condition. The inset shows the corresponding phase space trajectories.

the change in angle follows to first order as

$$\Delta\Theta_{\mathrm{x}} = \Theta_{\mathrm{x},1} - \Theta_{\mathrm{x}} = -S\sqrt{2J_{\mathrm{x}}}\cos^3(\Theta_{\mathrm{x}}) \ll 1$$

As a result, for the nonlinear betatron oscillation, the phase advance per turn

$$\tilde{\mu}_1 = 2\pi Q_{\mathrm{x}} - S\sqrt{2J_{\mathrm{x}}}\cos^3(\Theta_{\mathrm{x}})$$

shows an amplitude and phase dependent detuning.

As a particle with constant H revolves in phase space, the detuning term effectively modulates the betatron frequency as depicted in figure 1. This frequency modulation generates anharmonic motion and sidebands of higher order.

II. NONLINEAR BEAM SPECTRA UNDER EXCITATION

Spectra of transverse beam motion are obtained by observing the position of the circulating beam as a function of time at a fixed location in the synchrotron. For the linear case, the resulting spectra are well understood and dominated by the betatron sidebands at $f = (n \pm q_{\mathrm{x}})f_{\mathrm{rev}}$ below and above each harmonic $n \in \mathbb{N}$ of the revolution frequency f_{rev}. These sidebands are the result of an amplitude modulation of the transverse position caused by the betatron oscillations of particles and are used to determine linear quantities like tune and chromaticity [7].

In the nonlinear case the betatron oscillation are frequency modulated. Therefore, one expects multiple sidebands of order $k \in \mathbb{N}$ around each harmonic n:

$$f = (n \pm k\, q_{\mathrm{x}})\, f_{\mathrm{rev}}$$

A. Measurement of transfer function

A beam transfer function (BTF) measurement is performed by exciting the beam with a fixed frequency f_{ex} and observing the magnitude and phase of the induced beam oscillations filtered at that specific excitation frequency. The measurement is repeated within a single machine cycle for a range of frequencies, yielding the beam response as function of frequency. For a linear system the transfer function is well defined as the complex quotient of the observed and induced oscillation [8]. However, in the nonlinear case where the system response includes spectral components other than the excited frequency, the BTF can only show a subset of the beam oscillation frequencies present in the excited system [9].

Nevertheless, a BTF measurement can be used to probe the beam response at the frequency where the nonlinear sidebands of second order are expected. Such a measurement is presented in figure 2 for a typical RF-KO extraction setup from the Heavy Ion Synchrotron (SIS18) at GSI. Alongside the nonlinear case with sextupoles, also the linear case with sextupole magnets switched off is shown. As the closed orbit was not corrected, the sextupole magnets cause a tune shift. Therefore the location of the first and second order sidebands is indicated for both cases as obtained by fitting of the respective phase response.

A response of the beam to an excitation near the second order betatron sideband can only be observed for the nonlinear case with sextupoles switched on. The measurement demonstrates the existence of the second order sideband and the feasibility of exciting it. While the response is very weak compared to the first order sideband, one has to keep in mind that the BTF does not give insight into the beam oscillations at any but the excited frequency. For example, spectral components near the second order sideband induced by excitation at the first order sideband are not visible. However, the dip in the response at the first order sideband suggest, that in this case the primary oscillation frequencies are shifted away from the excitation frequency where the BTF is not sensitive [9]. Therefore, in the following, the beam motion is investigated by means of Schottky spectra in simulations.

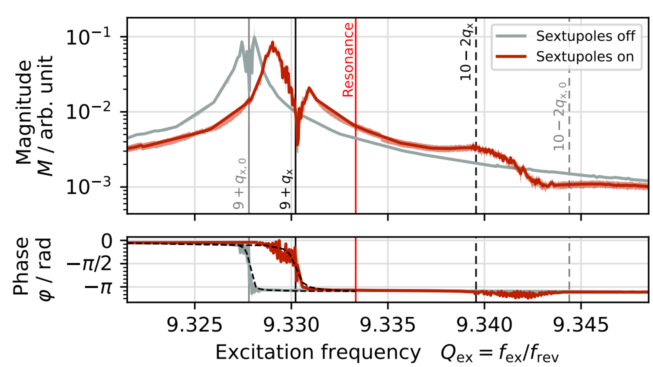

FIG. 2. Measured response to a sinusoidal excitation of varying frequency (BTF measurement) of an $^{197}Au^{65+}$ beam at 800 MeV/nucleon. Vertical lines indicate the location of the betatron sidebands and resonance.

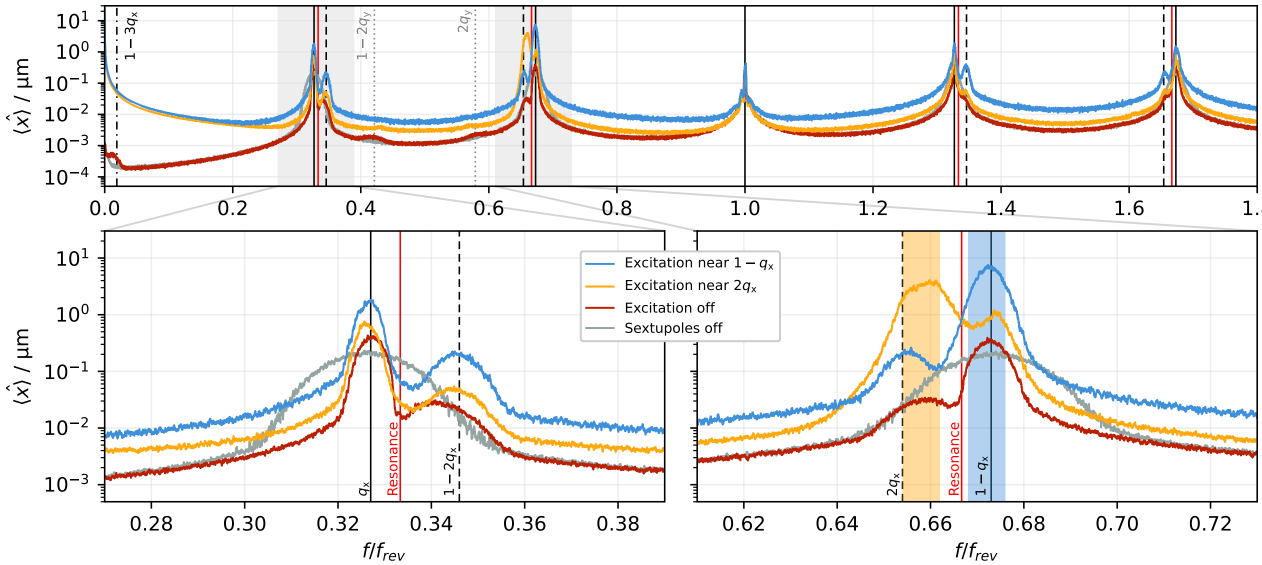

FIG. 3. Transverse Schottky spectra for the linear case (sextupoles off) and three nonlinear cases (sextupoles on) with and without excitation as obtained from a simulation. The zoom parts show beam oscillations at first and second order sidebands (vertical black lines) and at the excitation bands (yellow and blue shaded regions).

B. Simulation of Schottky spectra

Schottky diagnostics is a vital tool to study the incoherent particle motion by sampling the beam position at frequencies higher than the revolution frequency. Unlike the BTF, it provides a complete picture of the intrinsic beam oscillations independent of an external excitation. A particle tracking simulation is performed with Xsuite [10] for a typical machine setup of a Knock Out extraction from SIS18 at GSI. A beam of $^{238}U^{73+}$ ions with a rigidity of $B\rho = 7\,\mathrm{T\,m}$ and revolution frequency of $f_{\mathrm{rev}} = 785\,\mathrm{kHz}$ is prepared for extraction using a machine tune of $Q_{\mathrm{x,ref}} = 4.327$ and a corrected orbit.

Figure 3 shows the spectra of the horizontal beam centroid $\langle x \rangle$ as obtained from the simulation using a sampling frequency of $3.92\,\mathrm{MHz} = 5f_{\mathrm{rev}}$. In the linear case (sextupoles off), the regular betatron sidebands of first order are visible, which are relatively broad due to the large chromaticity of $\xi_{\mathrm{x}} = \Delta Q_{\mathrm{x}}/\delta = -6.6$. When the sextupoles are switched on for the purpose of slow extraction, the chromaticity reduces to $\xi_{\mathrm{x}} = -2.0$ and the first order sidebands become narrower. In addition, the sidebands of higher order ($k \geq 2$) become visible, most prominently the second order sidebands at $n \pm 2q_{\mathrm{x}}$. But also the weaker third order sideband at $1-3q_{\mathrm{x}} = 3|d| \approx 0$ and faint coupling bands at $n \pm 2q_{\mathrm{y}}$ can be observed. The latter are the result of the sextupole fields depending also on the vertical coordinate and therefore coupling the betatron motion in both planes.

In RF-KO extraction, the beam is excited transversely with a signal of a certain bandwidth. Under the excitation, the betatron oscillation amplitude is increased, and so does the magnitude in the respective Schottky spectra (figure 3). When the amplitude grows beyond the separatrix where particles are extracted, a significant DC leakage into the low frequencies is observed in the Schottky spectra due to the slow variation in centroid position compared to the case without extraction where the mean beam position remains at zero.

Traditionally, the excitation signal consists of a frequency band in the vicinity of one of the first order betatron sidebands. The excitation induces coherent beam oscillations at the excitation frequency, which can be observed in the Schottky spectrum. These are dominantly visible *only* at the *absolute* excitation frequency, and not at the other, not directly excited betatron sidebands. This becomes especially obvious for an excitation signal placed near the second order betatron sideband at $2q_{\mathrm{x}}$, for which the oscillation amplitude of the excited second order sideband is increased even beyond the amplitude of the nearby first order sidebands. This behaviour is only observed at the excited sideband, and not at the other sidebands in the Schottky spectrum, which are not directly excited. In general, the magnitudes in the Schottky spectrum for the case of excitation near the second order sideband are smaller compared to the excitation at the first order sideband with equal excitation strength. This suggests that the coupling to the beam is weaker at the higher order sidebands, but it is still sufficient for driving an RF-KO extraction.

III. KNOCK OUT EXTRACTION WITH SECOND ORDER SIDEBANDS

To study the effect of an excitation at a second order sideband on the RF-KO slow extraction process, the

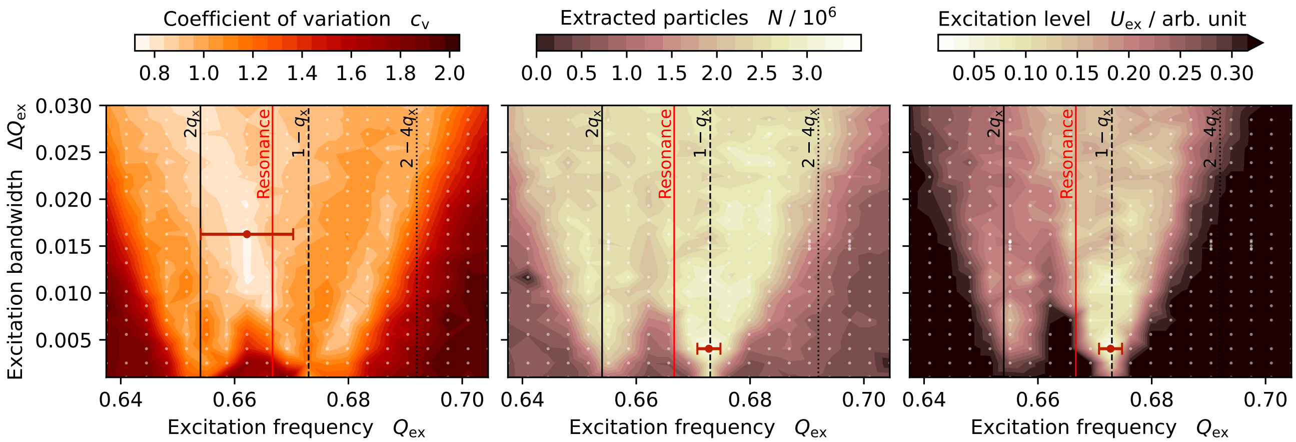

FIG. 4. Measured spill quality (left), number of particles extracted (middle) and required excitation strength (right) as a function of central frequency and bandwidth of a band-limited noise excitation signal. The spill quality is calculated for $\Delta t_{\mathrm{count}} = 100\,\mu\mathrm{s}$ and $\Delta t_{\mathrm{eval}} = 1\,\mathrm{s}$. White dots indicate the sampled points, and the red dot and span marks the respective global optimum and associated bandwidth. The vertical lines indicate the resonance and nearby betatron sidebands.

required excitation power and achievable spill quality is investigated.

The spill quality is given by the amount of unwanted intensity fluctuations in the time structure of the extracted beam. To quantify the fluctuations, the spill is divided into time intervals of length $\Delta t_{\mathrm{count}}$ and the number of extracted particles N is counted in each interval. The standard deviation $\sigma = \sqrt{\langle (N - \langle N \rangle)^2 \rangle}$ and mean $\mu = \langle N \rangle$, evaluated over a larger time span Δt_{eval}, is then used to determine the coefficient of variation c_{v} or the equivalent spill duty factor F [11]:

$$c_{\mathrm{v}} = \frac{\sigma}{\mu} = \sqrt{\frac{\langle N^2 \rangle}{\langle N \rangle^2} - 1} \qquad F = \frac{\langle N \rangle^2}{\langle N^2 \rangle} = \frac{1}{1 + c_v^2}$$

In addition to the spill quality, also the extraction efficiency is of importance. To extract all particles from the storage ring, a certain excitation power is required which depends strongly on the beam rigidity and the excitation signal used. In practice the available power of the RF amplification system can impose limits on the excitation signals which are feasible.

A. Machine measurement

The effects of excitation frequency and bandwidth on the RF-KO extraction are studied experimentally at the SIS18 of GSI. An $^{238}\mathrm{U}^{73+}$ beam with a kinetic energy of 200 MeV/nucleon (rigidity $B\rho = 7\,\mathrm{T\,m}$) is prepared and excited with a band-limited noise signal. The extracted spill is observed with a plastic scintillation based particle detector [12], which serves two purposes: First, the signal is used with a feedback system to dynamically adjust the excitation signal amplitude over the duration of the spill in order to maintain a constant spill rate [13]. Secondly, the intensity fluctuations measured by the detector are evaluated to determine the spill quality.

Figure 4 shows the results of a large scan of the excitation frequency and bandwidth, exceeding the traditionally used vicinity of the first order betatron sideband. The measurement proves, that RF-KO slow extraction by exciting the second order betatron sideband is possible, and a comparable number of particles can be extracted, namely $\langle N \rangle_{2q_x} / \langle N \rangle_{1-q_x} = 2.4(3)/2.7(3) = 90\,\%$. The excitation level required is with $\langle U_{\mathrm{ex}} \rangle_{2q_x} / \langle U_{\mathrm{ex}} \rangle_{1-q_x} = 0.21(4)/0.12(5) = 1.7(6)$ about twice as large as for the first order sideband. The optimal choice of excitation frequency and bandwidth from an efficiency point of view hence lies in the close vicinity of the first order betatron sideband.

However, the optimum in terms of spill quality was found on the opposite side of the resonance half way towards the second order betatron sideband (figure 4, left). Here, the measurement shows a reduction of the intensity fluctuations to $c_{\mathrm{v}} = 0.76$ compared to $c_{\mathrm{v}} = 1.21$ for the efficiency optimum at the first order sideband. This improvement in spill quality comes with an increased power requirement. While the transverse RF excitation system is capable of delivering these demands for the presented conditions, in general for higher rigidity beams a trade-off between spill quality and required power has to be found.

B. Simulation of spill quality

The previously introduced simulation code is used to model the machine experiment. Figure 5 shows the spill quality and required excitation power as a function of the excitation frequency as obtained from the simulation. Thereby, the bandwidth of the band-limited noise signal remains fixed. In agreement with the measure-

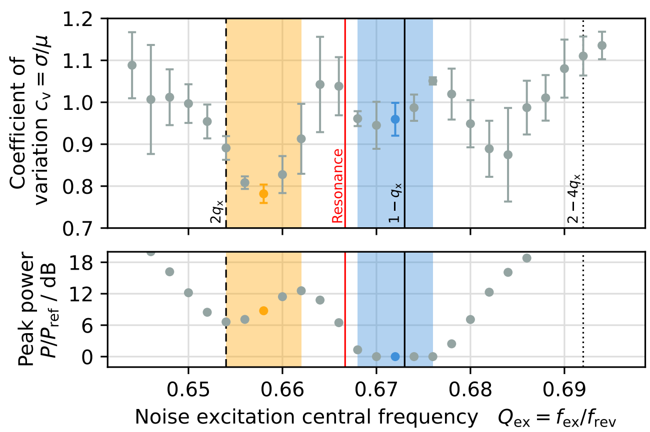

FIG. 5. Spill quality (top) and excitation power (bottom) as function of excitation frequency for a band-limited noise signal ($\Delta Q_{ex} = 0.008$) as obtained from simulations. The quality is calculated for $\Delta t_{count} = 100\,\mu s$ and $\Delta t_{eval} = 100\,ms$. Vertical lines mark the resonance and nearby betatron sidebands, and the two excitation bands from figure 3 are indicated.

ment, the global optimum in terms of spill quality is located on the opposite side of the resonance towards the second order betatron sideband. While the spill fluctuations are significantly reduced compared to an excitation band near the first order betatron sideband, the required excitation power is about 9 dB higher, corresponding to a factor three larger signal amplitude. The increase in the required excitation power is consistent with the experimental findings and the observations from the Schottky spectra discussed in the previous section.

Another local optimum can be found towards the fourth order betatron sideband $2 - 4q_x$, where the excitation power required is even higher. Once the power limit is reached, only a small fraction of the beam can be extracted and the value of $c_v \propto 1/\mu$ increases again.

C. Simulation of beam dynamics

To understand the mechanism behind the observed spill quality improvement, the beam dynamics is analysed in the particle tracking simulations. For the two excitation bands near the first and second order betatron sidebands discussed above, the particle distribution in horizontal phase space is recorded as a function of time, during the extraction. The Kobayashi Hamiltonian H normalized to its value at the separatrix $H_{sep} = (4\pi d)^3/S^2$ is used for a histogram of the particle distribution (figure 6). Thereby, $H = 0$ corresponds to a particle in the centre of phase space with zero betatron amplitude and (chromatic) tune Q_x; and for $H \to H_{sep}$ the betatron amplitude and nonlinear detuning increases (compare figure 1).

For both cases, the initial distribution is the same before the excitation is switched on at $t = 1.3\,ms$. The excitation band near $1 - q_x$ mainly couples to particles which perform linear betatron oscillations and are located in the core of the phase space. When these particles are excited by the band-limited signal, they diffuse outwards in phase space towards the separatrix, causing the distribution to become flatter (figure 6, top). This effectively increases the particle density in the vicinity of the separatrix, which makes the process more vulnerable to fluctuations of the separatrix size caused by power supply ripples [11]. It also intensifies fluctuations of the spill intensity caused by the diffusive nature of the noise excitation itself during the transition of particles across the separatrix. On the other hand, the excitation strength required to make particles cross the separatrix and become extracted is reduced.

In contrast, the excitation band near $2q_x$ can only couple to particles whose betatron oscillations are anharmonic and frequency modulated, since only then they have a spectral component at this frequency range. This applies to particles towards the separatrix which undergo amplitude and phase detuning (see section I A). As a result, the beam is "scraped off" from the outside and the phase space distribution becomes steeper towards the separatrix, while the particle density in the core at $H = 0$ is almost unaffected (figure 6, bottom). As the particle density in the vicinity of the separatrix does *not* increase during the slow extraction, spill intensity fluctuations are effectively reduced compared to the former case. However, it also means that a higher excitation strength is required to make particles from the core reach and cross the separatrix.

IV. CONCLUSION

The nonlinear particle dynamics at the 1/3 resonance used for resonant slow extraction induces a frequency modulation of betatron oscillations, which results in the appearance of additional betatron sidebands of higher order. The second order betatron sidebands are observed prominently in BTF measurements and Schottky spectra and can be used for transverse excitation of the beam. For RF-KO slow extraction, excitation of these second order sidebands requires a larger excitation power, but improves the spill quality significantly. As the excitation at the nonlinear second order band couples to particles near the separatrix, it effectively "scrapes off" the beam from the outside rather than pushing particles out from the inside of the phase space distribution. Thereby, accumulation of particles in the vicinity of the separatrix is avoided, reducing the vulnerability to processes diminishing the spill quality.

To improve the efficiency of the excitation process when sufficient power is not available, hybrid excitation signals can be used. For example, a weak noise-band at the $k = 1$ sideband feeding the extraction can be combined with a stronger excitation signal placed on the

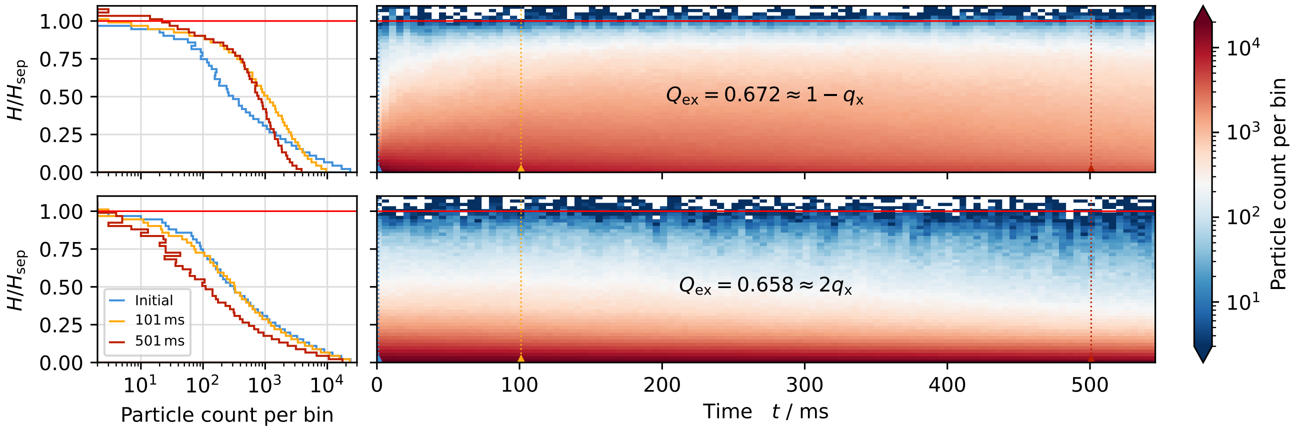

FIG. 6. Particle distributions before and during excitation near the first (top) and second order sideband (bottom) obtained from a simulation of 10^5 particles. The band-limited noise excitation signals correspond to figures 3 and 5 ($\Delta Q_{\rm ex} = 0.008$). The location of the separatrix at $H = H_{\rm sep}$ is indicated by the solid red line.

other side of the resonance towards the $k = 2$ sideband to benefit from the described spill quality improvement mechanism. This applies likewise to the components of more advanced excitation signals like Noise ++, a combination of a band-limited noise with sinusoidal excitation signals [14]. In figure 7 the spill quality is shown as a function of the frequency of the noise and one of the sine components of the Noise ++ excitation signal used at SIS18 at GSI for a $^{197}Au^{65+}$ beam at 200 MeV/nucleon. For the noise component, frequencies between the first order sideband and the resonance are detrimental to the spill quality, and it is preferable to place the noise band at a sufficient distance to the $1 - q_{\rm x}$ band or on the other side of the resonance. For the frequency of the sine component a local optimum exists not only at $Q_{\rm ex,1} = 0.677 = 1 - 0.323$ towards the first order sideband, but also at $0.648 = 2 \cdot 0.324$ towards the second order sideband on the other side of the resonance. With $1 - q_{\rm x} = 2/3 + |d|$ and $2q_{\rm x} = 2/3 - 2|d|$ the observed behaviour on the left side of the resonance is essentially a mirror image of the right side, scaled by a factor of two.

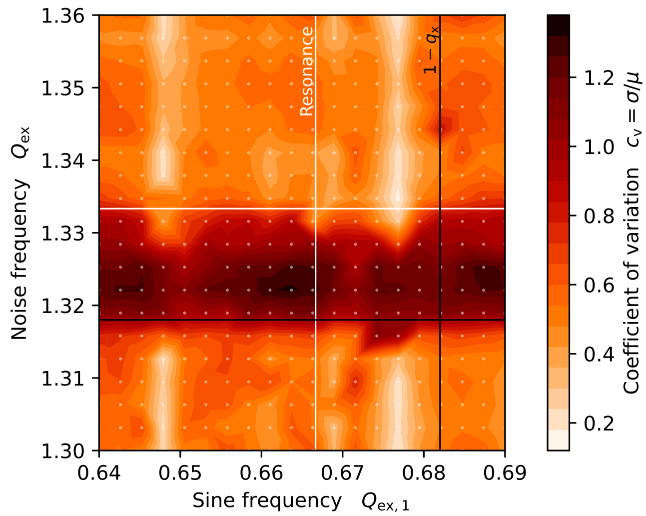

FIG. 7. Measured spill quality as a function of sine and noise frequency for an excitation with Noise ++. For the scan, the noise bandwidth $\Delta Q_{\rm ex} = 0.01$ and frequency of the second sine $Q_{\rm ex,2} = 1.6715$ are kept constant.

In general, finding the optimal excitation frequencies is an optimization problem. By setting appropriate boundaries, one can allow the optimization algorithm to explore also the region of the second order sideband and then chose the local optimum according to the available excitation power.

ACKNOWLEDGMENTS

The beam instrumentation department at GIS is acknowledged for the support in carrying out the measurements. We thank C. Cortés for valuable discussions on nonlinear BTF measurements.

[1] K. Hiramoto and M. Nishi, Resonant beam extraction scheme with constant separatrix, Nucl. Instrum. Methods Phys. Res., Sect. A **322**, 154 (1992).
[2] M. Tomizawa, M. Yoshizawa, K. Chida, J. Yoshizawa, Y. Arakaki, R. Nagai, A. Mizobuchi, A. Noda, K. Noda, M. Kanazawa, A. Ando, H. Muto, and T. Hattori, Slow beam extraction at tarn ii, Nucl. Instrum. Methods Phys. Res., Sect. A **326**, 399 (1993).
[3] M. Benedikt, P. J. Bryant, L. Badano, M. Crescenti, P. Holy, A. T. Maier, M. Pullia, S. Rossi, and P. Knaus,

Proton-Ion Medical Machine Study (PIMMS): Part I, Tech. Rep. CERN/PS 99-010 (DI) (Geneva, 1999).

[4] A. Franchi, L. Farvacque, F. Ewald, G. Le Bec, and K. B. Scheidt, First simultaneous measurement of sextupolar and octupolar resonance driving terms in a circular accelerator from turn-by-turn beam position monitor data, Phys. Rev. ST Accel. Beams **17**, 074001 (2014).

[5] C. Belver-Aguilar, A. Faus-Golfe, F. Toral, and M. J. Barnes, Stripline design for the extraction kicker of compact linear collider damping rings, Phys. Rev. ST Accel. Beams **17**, 071003 (2014).

[6] Y. Kobayashi, Theory of the resonant beam ejection from synchrotrons, Nuclear Instruments and Methods **83**, 77 (1970).

[7] M. Betz, O. R. Jones, T. Lefevre, and M. Wendt, Bunched-beam schottky monitoring in the lhc, Nucl. Instrum. Methods Phys. Res., Sect. A **874**, 113 (2017).

[8] J. Borer, G. Guignard, A. Hofmann, E. Peschardt, F. Sacherer, and B. Zotter, Information from beam response to longitudinal and transverse excitation, IEEE Trans. Nucl. Sci. **26**, 3405 (1979).

[9] E. C. Cortés García, P. Niedermayer, R. Singh, R. Taylor, E. Benedetto, E. Feldmeier, M. Hun, and T. Haberer, Interpretation of the horizontal beam response near the third integer resonance, preprint.

[10] G. Iadarola, R. D. Maria, S. Łopaciuk, A. Abramov, X. Buffat, D. Demetriadou, L. Deniau, P. D. Hermes, P. Kicsiny, P. Kruyt, A. Latina, L. Mether, K. Paraschou, G. Sterbini, F. F. Van der Veken, P. Belanger, P. Niedermayer, D. Di Croce, T. Pieloni, L. van Riesen-Haupt, and M. Seidel, Xsuite: An integrated beam physics simulation framework.

[11] R. Singh, P. Forck, P. Boutachkov, S. Sorge, and H. Welker, Slow extraction spill characterization from micro to milli-second scale, J. Phys. Conf. Ser. **1067**, 072002 (2018).

[12] P. Forck, T. Hoffmann, and A. Peters, Detectors for slowly extracted heavy ions at the gsi facility, in *Proc. DIPAC'97*, European Workshop on Diagnostics and Instrumentation for Particle Accelerators (INFN-LNF, Frascati, Italy, 1997) pp. 165–167.

[13] P. J. Niedermayer, R. Singh, and R. Geißler, Software-defined radio based feedback system for beam spill control in particle accelerators, in *Proc. GRCon23*, GNU Radio Conference (GNU Radio Journal, Tempe, AZ, USA, 2023).

[14] P. Niedermayer and R. Singh, Excitation signal optimization for minimizing fluctuations in knock out slow extraction, preprint (2024).